ELSEVIER

Chemical Engineering Science 60 (2005) 151–166

Chemical Engineering Science

www.elsevier.com/locate/ces

Mass transfer enhancement in the Membrane Aromatic Recovery System (MARS): theoretical analysis

Frederico C. Ferreira, Ludmila G. Peeva, Andrew G. Livingston*

Department of Chemical Engineering and Chemical Technology, Imperial College—London, London SW7 2AZ, UK

Received 4 March 2004; received in revised form 26 July 2004; accepted 28 July 2004
Available online 17 September 2004

Abstract

This work investigates three different models describing mass transfer enhancement by a reversible and instantaneous second-order chemical reaction. The three models are applied to the study of mass transfer phenomena occurring in a membrane process for recovery of organic chemicals, the Membrane Aromatic Recovery System (MARS). Typical MARS operating conditions are used as model inputs, and the results obtained are used to assess the degree of complexity that should be taken into account in describing the mass transfer phenomena. The most complex model derived (N–P model) accounts for chemical reaction reversibility and the Nernst–Planck effect created by ionic species and is solved numerically. Following Olander model for a second order reversible instantaneous reaction model is proposed, for which we derive an analytical solution in terms of bulk solution properties. Finally, the simplest model follows the analysis of Hatta, assuming irreversible chemical reaction and neglecting the Nernst–Planck effect. The reversibility of the reaction is shown to be important, while N–P effects are negligible. The Olander model is recommended for use in describing the mass transfer phenomena. The models developed can be applied further to other processes of similar type.

Keywords: Mass transfer; Mathematical modelling; Chemical reaction; Enhancement; Membrane; Extraction

1. Introduction

In chemical engineering processes, mass transfer phenomena often take place accompanied by chemical reaction, particularly in operations involving gas absorption, extraction, ion exchange and more recently membrane technology (Noble, 1991; Van Swaaij and Versteeg, 1992; Cussler, 1997; Al-Marzouqi et al., 2002). Chemical reaction can greatly enhance mass transfer rates (Cussler, 1997), dramatically reducing the operational interfacial area required, which can translate into important savings in the chemical plant construction and operating costs. Among the great variety of chemical engineering processes in which chemical reaction and mass transfer are coupled, in this paper we have chosen to focus on the Membrane Aromatic Recovery System (MARS).

MARS was first applied to the recovery of phenol (Han et al., 2001) and aniline (Ferreira et al., 2002a) from synthetic wastewaters at laboratory scale. The aniline and phenol compound families usually have high boiling points and low vapour pressures, therefore the existing separation processes that rely on liquid–gas phase transitions, such as distillation and pervaporation, have high-energy requirements. Also, the intermediate polarity of these compounds creates problems with phase separation and contamination in solvent extraction. Hence MARS was developed as a new membrane process for recovery of organic acids and bases from industrial wastewater streams.

The first MARS pilot scale unit was applied to recover aniline from an industrial wastewater effluent arising in a 4-nitrodiphenyl production process (Ferreira et al., 2002b) and has recently been commercialised at a large scale (Chin,

* Corresponding author. Tel.: +44-20-7594-5582; fax: +44-20-7594-5629.
E-mail address: a.livingston@imperial.ac.uk (A.G. Livingston).

0009-2509/$ - see front matter © 2004 Elsevier Ltd. All rights reserved.
doi:10.1016/j.ces.2004.07.081

2003). The final product purity was high enough to allow for recycling into the chemical production process.

An accurate mathematical description of mass transfer in the MARS process, which could be used further for predictive purposes and scaling up, is a key priority in the further development of this technology and the main objective of the present study. This paper considers the transport phenomena involved and relevant models, and shows the simplest model which is capable of dealing with all relevant phenomena. A subsequent paper will investigate these models experimentally.

2. Theoretical background

2.1. The process

The MARS process comprises two stages as shown in Fig. 1 (Han et al., 2001; Ferreira et al., 2002a,b). In the first stage an organic acid or base is extracted from a wastewater (feed side), through a non-porous membrane, into a stripping solution, where it is accumulated in its ionic form. In the second stage, the stripping solution, loaded with ionised organic at high concentration is neutralised, and the organic recovered. In MARS, the reactant solution is the stripping solution, where the organic can exist in two forms, the transported neutral solute (A) and the ionic reaction product (AB). The reactant solute (B) is either a hydroxide or hydronium ion and therefore is directly related to the stripping solution pH. The chemical reaction in the stripping solution is a reversible second-order reaction of the Brönsted acid–base type, and can be considered instantaneous compared to the mass transfer rates involved in the process. The membrane is a solid non-porous polymer, usually silicone rubber, impermeable to ionic species, and thus the chemical reaction does not occur inside the membrane. The membrane mass transfer resistance is determined by the membrane permeability (Ferreira et al., 2002a,b) and is independent of the chemical reaction. When the membrane resistance is dominant in the overall mass-transfer resistance of the MARS process, the enhancement effect of the chemical reaction can be neglected. In all other cases the chemical reaction enhancement factor should be considered.

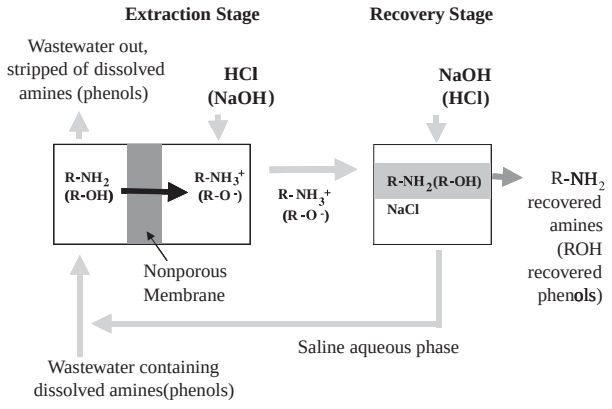

Fig. 1. Schematic diagram of MARS process. Brackets show the alternative compound.

2.2. Models for instantaneous reaction with mass transfer

One of the first authors who mathematically described mass transfer enhancement due to chemical reaction was Hatta, in 1928 (Hatta, 1928, 1932). This model applies stagnant liquid film theory and considers an instantaneous and homogenous irreversible chemical reaction. The use of instantaneous chemical reaction avoids the inclusion of kinetic parameters and results in a mass transfer model of an attractive mathematical simplicity, in particular for second-order irreversible chemical reactions. The Hatta model was first developed for gas absorption processes, without taking into account the effect of ionic diffusion. However, several reactions, including Brönsted acid–base reactions occurring in the MARS process and some phase transfer catalyst reactions (Noble, 1991), involve ionic reactants and products, and for such cases the Nernst–Planck effect can be important and can significantly influence the transfer rate of the ionic species. Sherwood and Wei (1955) and later, Brian et al. (1964), addressed this problem for irreversible reactions and obtained an analytical solution, taking into account both concentration and electric field driving forces, and imposing the electroneutrality condition throughout the reactant solution liquid film. Grosjean and Sawistowski (1980) applied these models to a liquid/liquid system, in which propionic acid is extracted from a toluene phase to a dilute aqueous caustic solution. The MARS process involves mono-valent ionic species which potentially lead to Nernst–Planck effects, which will be considered in this work.

The above studies assumed that the chemical reaction is irreversible. This assumption was adequate, since the transported solute concentration was negligibly low in the reactant bulk solution and hence the reverse step of the chemical reaction could be ignored in the mass transfer phenomena. Such a scenario prevails for concentrations of reactant (B) high enough, and product (AB) low enough, to shift the chemical equilibrium towards the product. However, the opposite scenario prevails in MARS: (i) the concentration of the organic in the bulk stripping solution has to be high enough to allow for recovery in the MARS recovery stage, implying high product concentrations (normally above 2 M); and (ii) the concentration of ionic reactant (B) is constricted at values below 0.1 M in the operating stripping solution, i.e. within a pH range from 1 to 13, since it is only in this region that the membrane materials have acceptable chemical resistance. Therefore, at the MARS operating conditions, depending on the equilibrium constant, the neutral organic concentration (A) in the bulk stripping solution is usually not negligible. Typically,

it is in the range of ∼ 0.002 M while the mass transfer driving force range varies within ∼ 0.5 to ∼ 0.005 M, and so the chemical reaction reversibility plays an important role in mass transfer enhancement.

Olander (1960) has derived a model, which describes the effect of a second-order instantaneous chemical reaction on mass transfer enhancement taking into account reversible chemical reaction. This model imposes the condition of chemical reaction equilibrium throughout the liquid film and the bulk reactant solution. However, the Olander model has been derived for neutral species and therefore neglects the Nernst–Planck effect. The analytical solution presented in Olanders' work includes a chemical reaction mass transfer enhancement factor dependent on the transported solute (A) concentration at the interface between the inert and the reactant phases. However, this concentration is not expressed explicitly in terms of measurable variables. A detailed literature review on the applications of the Olander model to mass transfer in liquid membranes can be found elsewhere (Al-Marzouqi et al., 2002). Modifications of the Olander model using penetration and surface renewal theories have also been developed; however the solutions found were very similar independently of the mass transfer theory applied (Astarita and Savage, 1982). Therefore, in the present work the liquid film theory also will be used.

This work presents a mathematical analysis of the mass-transfer in the MARS process from the point of view of the three foregoing models. A model (N–P) for chemical reaction mass transfer enhancement accounting for the Nernst–Planck effect and reversible chemical reaction is developed. A new analytical solution for the Olander model, expressed entirely in bulk solution (i.e. measurable) variables and parameters, is also proposed. Typical MARS operating conditions were used as inputs for the N–P, Olander and Hatta models presented and the solutions were compared. The aim of this work is to identify if or when the Nernst–Planck effect and chemical reaction reversibility are important for the MARS and under which conditions a simpler model can be used to give accurate predictions of mass transfer enhancement.

3. Mathematical analysis

The following assumptions are used in the three different models derived here:

1. Instantaneous chemical reaction of second order occurs in the stripping solution with the general expression:

   $$A + B \rightleftharpoons AB.$$

   where A is the specie transported across the membrane, B is the reactant in the stripping solution, AB is the reaction product (for the MARS process A is typically phenol or aniline, B hydroxide or hydronium and AB phenolate or anilinium)
2. Reaction reversibility is assumed for Olander and N–P models, while in the Hatta model an irreversible reaction is considered.
3. The membrane is impermeable to water and ionic species.
4. Liquid film theory is applied for the case of steady-state process, i.e. all the variables are time independent.
5. Flat plane geometry (coordinates) have been used in this work. Even though the membrane tube used is cylindrical, for small ratios between liquid film thickness and membrane tube radius a flat plane geometry can be assumed (Cussler, 1997).
6. Activity coefficients of all the species are assumed to be unity.
7. Diffusion and partition coefficients of the neutral organic species are assumed to be concentration independent constants.

3.1. Mathematical description of MARS according to the N–P model: reversible second-order chemical reaction with Nernst–Planck effect

This model takes into account the chemical reaction reversibility and the Nernst–Planck effect. This last effect quantifies the existence in solutions of charged species moving with different velocities due to their different ionic diffusion coefficients, and therefore generating an instantaneous electric potential (field) and corresponding electric driving force. The latter has to be considered in addition to the concentration driving force. The flux equation for each of the ionic species can be expressed as follows:

$$\phi_j = \frac{J_j}{I_m} = -D_j.\frac{\mathrm{d}C_j}{\mathrm{d}x} + z_j \Psi D_j.C_j \tag{1}$$

When the counter ion (C^*) is taken into account, a Bröntsed acid base reaction actually involves four species: A is a neutral specie (for example phenol), B the monoionic reactant (for example hydroxide), AB the product (for example phenolate) and C^* the counter ion (for example sodium):

$$\begin{aligned} A + [C^*B] &\rightleftharpoons [C^*AB] \\ &\text{e.g. } \mathrm{PhOH} + \mathrm{Na^+OH^-} \\ &\rightleftharpoons \mathrm{Na^+PhO^-} + \mathrm{H_2O} \end{aligned} \tag{2}$$

In order to fulfil the electroneutrality requirements, two more equations representing the ionic concentration balance and the net current flux balance have to be added to the system:

$$\sum_j z_j.C_j = 0 \Rightarrow C^* = B + AB \tag{3}$$

$$\sum_j z_j.J_j = 0 \Rightarrow J_{C^*} = J_B + J_{AB} \tag{4}$$

The commonly used mathematical solution for this problem, as for example presented by Brian (Brian et al., 1964), is to

substitute Eq. (1) into Eq. (4), and thus obtain an expression for the electric field (Eq. (5)).

$$\Psi = \frac{F}{\mathrm{RT}}.V = \frac{\sum_j z_j.D_j \frac{\mathrm{d}C_j}{\mathrm{d}x}}{\sum_j z_j^2.D_j.C_j} \Rightarrow$$

$$\Psi = \frac{z_{C^*} D_{C^*} \frac{\mathrm{d}C^*}{\mathrm{d}x} + z_B D_B \frac{\mathrm{d}B}{\mathrm{d}x} + z_{AB} D_{AB} \frac{\mathrm{d}AB}{\mathrm{d}x}}{z_{C^*}^2.D_{C^*}.C^* + z_B^2 D_B.B + z_{AB}^2 D_{AB}.AB}. \quad (5)$$

For the present system, all the species are mono valent (i.e. $z_j = \pm 1$). The counter ion concentration can be eliminated from the electric field expression by substituting Eq. (3) into Eq. (5):

$$\Psi = z_{C^*}.\frac{\frac{\mathrm{d}B}{\mathrm{d}x}(D_{C^*} - D_B) + \frac{\mathrm{d}AB}{\mathrm{d}x}(D_{C^*} - D_{AB})}{B.(D_{C^*} + D_B) + AB.(D_{C^*} + D_{AB})}. \quad (6)$$

The final electric field expression (Eq. (6)) can be substituted back into Eq. (1) to obtain an expression for the different species fluxes. Similarly to the Olander model (Olander, 1960), a system of equations including the mass balances for the fluxes with chemical reaction consumption/production, and the equation for instantaneous chemical equilibrium, is established.

$$D_A.\frac{\mathrm{d}^2A}{\mathrm{d}x^2} + D_{AB}.\frac{\mathrm{d}^2AB}{\mathrm{d}x^2} - z_{AB}.D_{AB}.\frac{\mathrm{d}(\Psi.AB)}{\mathrm{d}x} = 0, \quad (7)$$

$$D_B.\frac{\mathrm{d}^2B}{\mathrm{d}x^2} - z_B.D_B.\frac{\mathrm{d}(\Psi.B)}{\mathrm{d}x} + D_{AB}.\frac{\mathrm{d}^2AB}{\mathrm{d}x^2} - z_{AB}.D_{AB}.\frac{\mathrm{d}(\Psi.AB)}{\mathrm{d}x} = 0, \quad (8)$$

$$AB = K.B.A. \quad (9)$$

To this system of equations is added a set of boundary conditions, presented in the appendix. The numerical solution of the system allows calculation of the different species concentration profiles and enhanced fluxes. Details can be found in the appendix. In the stripping solution the organic compound can exist in two forms, the neutral reagent and the ionic product, therefore the total organic flux is the sum of the fluxes of these two species:

$$\phi_{\mathrm{ov}} = \phi_A + \phi_{AB} = -D_A.\frac{\mathrm{d}A}{\mathrm{d}x} - D_{AB}.\frac{\mathrm{d}AB}{\mathrm{d}x} + z_{AB}.D_{AB}.\Psi.AB \quad (10)$$

3.2. Mathematical description of MARS according to the Olander model: reversible second-order reaction for neutral species

As already mentioned the Olander model was derived for neutral species, and ignores any resultant electric fields. This model takes into account the reversibility of the chemical reaction and allows for a significant concentration of the neutral organic in the bulk stripping solution ($A_{s,b}$). The system of differential equations proposed by Olander can be considered as a particular case of the N–P model, where the electroneutrality equations are excluded and a value of zero is given to the electric field, which implies that the only driving force for the mass-transfer is the concentration driving force.

When only the concentration driving force is taken into account, the organic flux can be calculated as a function of the bulk concentration driving force and the overall mass transfer coefficient.

$$J_{\mathrm{ov}} = I_m.K_{\mathrm{ov}}.(A_{f,b} - A_{s,b}) \quad (11)$$

The resistances-in-series approach is used to describe the overall mass transfer coefficient and three mass transfer resistances are considered for the system: (i) the feed liquid film resistance, (ii) the membrane resistance, and (iii) the stripping liquid film resistance. The membrane resistance accounts for the organic diffusion coefficient (D_m) inside the membrane material, the membrane thickness (δ_m) and the organic partition coefficient (K_p) between the membrane material and the feed aqueous phase. The feed and the membrane resistances are independent of the chemical reaction effect; hence for mathematical simplification they are grouped in a single resistance ($1/k_g$), expressed in Eq. (12).

$$\frac{1}{k_g} = \frac{1}{k_f} + \frac{1}{k_m} = \frac{1}{k_f} + \frac{\delta_m}{D_m.K_p}. \quad (12)$$

The overall mass transfer coefficient is then defined in Eq. (13)

$$\frac{1}{K_{\mathrm{ov}}} = \frac{1}{k_g} + \frac{1}{E.k_s^0}, \quad (13)$$

E is an enhancement factor, which expression depends on the model used. When chemical reaction does not take place $E = 1$, and the overall mass transfer will be denoted K_{ov}^o and the organic flux J_{ov}^o.

The original expression for the enhancement factor presented by Olander is:

$$E = 1 + \frac{D_{AB}}{D_A}.\frac{K.B_{s,b}}{1 + \frac{D_{AB}}{D_B}K.A_{s,i}}. \quad (14)$$

However, as already mentioned, this expression contains the membrane/stripping solution interfacial concentration of the neutral organic $A_{s,i}$, an interfacial variable, which cannot be easily measured experimentally and is not easily expressible as function of the system operating parameters.

As for the N–P model, the Olander model can be solved numerically, using the system of differential equations and boundary conditions presented in the appendix, and the organic flux calculated from Eq. (10) (but with z equals to zero). The Olander model, as applied to the MARS process, can also be solved analytically. In this approach the membrane/stripping interface organic concentration is calculated

from Eq. (15), derived in this study

$$A_{s,i} = \frac{-b + \sqrt{b^2 - 4ac}}{2a}, \tag{15}$$

where,

$$a = \left(1 + \frac{k_g}{k_s^0}\right).\frac{D_{AB}}{D_B}K,$$

$$b = \left(1 + \frac{k_g}{k_s^0}\right) + \frac{D_{AB}}{D_A}K.B_{s,b} - \left(A_{s,b} + \frac{k_g}{k_s^0}.A_{f,b}\right).\frac{D_{AB}}{D_B}K,$$

$$c = -\left[\frac{k_g}{k_s^0}A_{f,b} + A_{s,b}.\left(1 + \frac{D_{AB}}{D_A}K.B_{s,b}\right)\right].$$

Details of this derivation can be found in the appendix. The expression for the interfacial concentration (Eq. (15)) derived is then replaced in the Olander enhancement factor (Eq. (14)). Thus the overall mass transfer coefficient (Eq. (13)) and the respective organic flux for a given concentration driving force (Eq. (11)) can be calculated.

3.3. Mathematical description of MARS according to the Hatta model: irreversible second-order reaction

Following Hatta's work, a simple model was applied for the mass transfer in MARS process. This model also considers an organic flux based on the overall mass transfer coefficient (Eqs. (11) and (13)). However it is assumed that the chemical reaction is irreversible and therefore the neutral organic concentration ($A_{s,b}$) in the bulk stripping solution is zero. Mechanistically, the transported solute (A) and the reactant solute (B) enter and diffuse in the stagnant film from opposite directions, meeting each other at the reaction plane, where they react and are completely converted into reaction product (AB). The well known Hatta enhancement factor is defined in Eq. (16):

$$E = 1 + \frac{D_B}{D_A}.\frac{B_{s,b}}{A_{s,i}}. \tag{16}$$

The membrane/stripping solution interfacial concentration can be calculated from Eq. (17), derived in the appendix.

$$A_{s,i} = \frac{\frac{k_g}{k_s^0}.A_{f,b} - \frac{D_B}{D_A}.B_{s,b}}{\left(1 + \frac{k_g}{k_s^0}\right)}. \tag{17}$$

Further mathematical manipulation of the Hatta model equations, allows the mass transfer enhancement to be expressed in terms of a flux ratio:

$$\frac{J_{ov}}{J_{ov}^0} = \frac{K_{ov}}{K_{ov}^0} = 1 + \frac{D_B}{D_A}.\frac{B_{s,b}}{A_{f,b}}, \tag{18}$$

$$J_{ov} = I_m.\left[1 + \frac{D_B}{D_A}.\frac{B_{s,b}}{A_{f,b}}\right].K_{ov}^0.A_{f,b}. \tag{19}$$

However, Eqs. (18) and (19) are valid only for mass transfer enhancement values lower than the maximum possible chemical reaction enhancement, i.e. for the cases when $K_{ov} < k_g$. When the reaction front reaches the membrane/stripping solution interface, the stripping solution mass transfer resistance is completely eliminated; the maximum flux enhancement is reached (i.e. in Eq. (13) for $E \to \infty$, $K_{ov}^{Max} = k_g$), as quantified by Eqs. (20) and (21):

$$\frac{J_{ov}^{Max}}{J_{ov}^0} = \frac{K_{ov}^{Max}}{K_{ov}^0}\frac{A_{f,b}}{A_{f,b}} = \frac{\frac{1}{k_g} + \frac{1}{k_s}}{\frac{1}{k_g}} = 1 + \frac{k_g}{k_s^0}, \tag{20}$$

$$J_{ov}^{Max} = I_m.k_g.A_{f,b}. \tag{21}$$

Details on the derivation of expressions 16–19 can be found in the appendix. For a given feed solution bulk concentration $A_{f,b}$, a critical stripping solution bulk concentration of the reactant B, above which the enhancement is maximum, can be calculated. The Hatta model prediction for such a concentration is given by Eq. (22).

$$B_{s,b}^{critical} = \frac{k_g}{k_s^0}\frac{D_A}{D_B}A_{f,b}. \tag{22}$$

A summary of the basic ideas of the three models is presented in Fig. 2.

4. Model input values and MARS operating parameters

The input parameters for the three models are summarised in Table 1. These inputs can be categorised into three groups: (i) the chemical compound properties, (ii) the system mass transfer properties and (iii) the operating parameters. The parameters in the first two groups are determined by the nature of the system and cannot be altered freely.

4.1. Chemical compound properties

The chemical compound properties required for these models are chemical and physical constants, such as diffusion coefficients, the water auto-ionisation constant (K_w) and the organic acid dissociation constant (K_a) all available in the literature. The equilibrium constant is directly related to K_a. For organic bases or acids it is calculated as:

$$K = \frac{C_{RNH_3^+}}{C_{RNH_2}.C_{H_3O^+}} = \frac{1}{K_a} \quad \text{or}$$

$$K = \frac{C_{RO^-}}{C_{ROH}.C_{OH^-}} = \frac{1}{K_b} = \frac{K_a}{K_w}. \tag{23}$$

The main aim of the present paper is a theoretical comparison between the three models, and the analysis is applied only to phenol as a model compound and only phenol physical and chemical properties (diffusion coefficients and K_a) are used in this study. Experimental model testing and extension towards other compounds and conditions will be presented in subsequent paper.

4.2. System mass transfer properties

The system mass transfer properties are defined by the three mass transfer coefficients: k_f, k_m and k_s. The values for

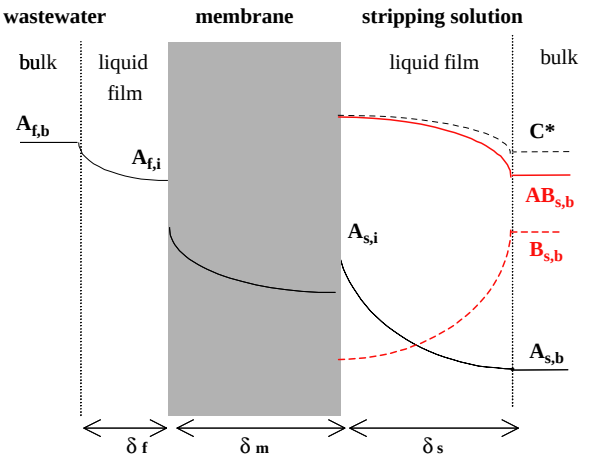

N-P model

-Reversible reaction.
-Allows for existence of neutral organic concentration in stripping solution

-Charged species Nernst-Planck effect.
-Includes counterion (C*) diffusion in the model.

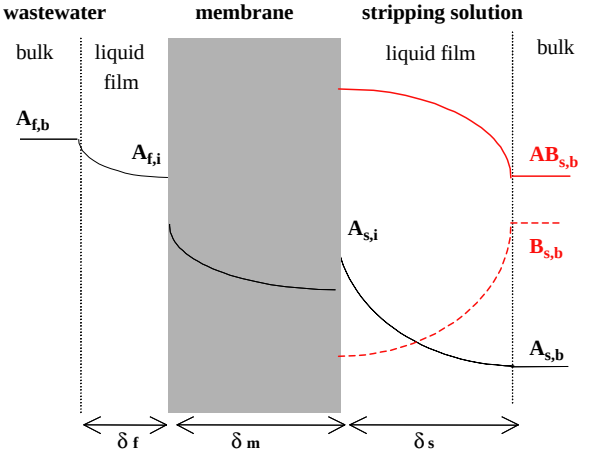

Olander model

-Reversible reaction.
-Allows for existence of neutral organic concentration in stripping solution

-Neutral species Nernst-Planck effect neglected
-Counter ion diffusion is not included.

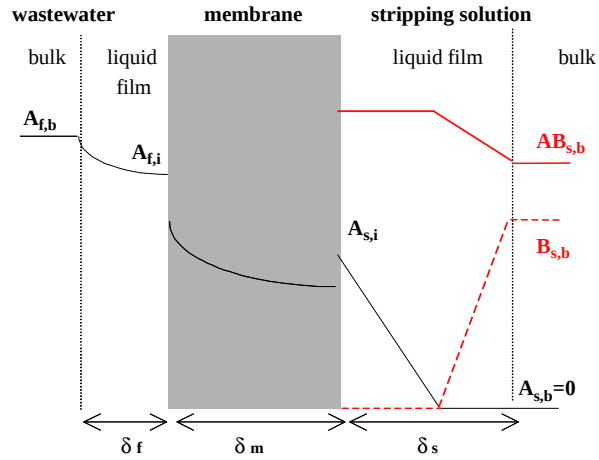

Hatta model

-Irreversible reaction.
-Neutral organic concentration in the stripping solution is zero.

-Neutral species Nernst-Planck effectneglected.
-Counter ion diffusion is not included.

Fig. 2. Schematic representations of concentration profiles in each of the three models.

the system mass transfer parameters were determined from independent experiments as described elsewhere (Ferreira, 2004). As could be expected, the stripping liquid film mass-transfer coefficient (k_s) depends strongly on the hydrodynamic conditions, system configuration, operating scale and stripping solution viscosity (Ferreira, 2004). In this paper a value of 8.9×10^{-7} m s^{-1} was chosen, as typical for the MARS operations at lab scale (Ferreira, 2004). The liquid film thickness (δ) is also required as a parameter for the numerical solutions; the value used (1 mm) was evaluated from

Table 1
Model inputs

	Variable description	Units	Model	Range/Value
M_w	Organic molecular weight	$g\,mol^{-1}$	I, II, III	94
M_w^{add}	Ionic reagent molecular weight	$g\,mol^{-1}$	I, II, III	40
k_g	"Grouped" mass transfer coefficient (includes membrane and liquid film feed resistances)	$m\,s^{-1}$	I, II, III	Case *L*: 2×10^{-7} Case *H*: 5×10^{-7}
k_s^0	Stripping solution liquid film mass transfer coefficient	$m\,s^{-1}$	I, II, III	8.9×10^{-7}
$B_{s,b}$	Stripping solution bulk ionic concentration. Corresponds actually to a stripping pH value	M	I, II, III	10^{-1}–10^{-3}; pH = 11–13
$A_{f,b}$	Feed bulk organic concentration in wastewater	M	I, II, III	10^{-1}–10^{-4}
D_A	Neutral organic diffusion coefficient	$m^2\,s^{-1}$	I, II, III	0.89×10^{-9}
D_B	Ionic reagent diffusion coefficient	$m^2\,s^{-1}$	I, II, III	5.3×10^{-9}
D_{AB}	Ionic organic diffusion coefficient	$m^2\,s^{-1}$	II, III	0.86×10^{-9}
K	Equilibrium constant (from pK_a and pK_w)	M^{-1}	II, III	10^4
C^{Add}	Ionic reagent (NaOH or HCl) concentration added to stripping solution (controls $C_{s,b}^T$ at steady state)	(wt%)	II, III	10
D_{C^*}	Counter ion diffusion coefficient	$m\,s^{-2}$	III	1.33×10^{-9}

the fundamental definition of k_s, for the flat plane geometry:

$$k_s = \frac{D_A}{\delta}. \tag{24}$$

Typically MARS operates in the laminar hydrodynamic regime due to the restrictions of high pressure drop down the membrane tube (Ferreira et al., 2004); therefore the feed liquid film mass-transfer coefficients are in the range of $10^{-6}\,m\,s^{-1}$. The mass transfer coefficients of phenol through the silicone rubber membrane are in the range of $10^{-7}\,m\,s^{-1}$. However in order to improve the MARS process performance, an ongoing program of research seeks new membranes with higher phenol permeability (mass transfer in the range of $10^{-6}\,m\,s^{-1}$) suitable for MARS applications. Therefore to consider this second opportunity, the model calculations were performed for two membrane permeability case studies: a membrane with a low organic flux, corresponding to the current MARS process k_g value of $2 \times 10^{-7}\,m\,s^{-1}$ (Case *L*) and a membrane with a high organic flux corresponding to a k_g value of $5 \times 10^{-7}\,m\,s^{-1}$(Case *H*). In this latter case both the membrane and the feed liquid film mass transfer coefficient were assumed to be $1.0 \times 10^{-6}\,m\,s^{-1}$.

4.3. Operating parameters

The input operating parameters include different concentrations. The bulk feed concentration ($A_{f,b}$) in the real MARS operation is a time or space dependent variable (for a batch or continuous configuration, respectively) and its value will vary between the industrial waste stream concentration and the target concentrations for discharge. However, in this work our interest is in the mass transfer phenomena, and for each individual simulation, the bulk feed concentration ($A_{f,b}$) is fixed at a single value. To evaluate effects on MARS process performance a wide range of phenol concentrations were considered (0.5–5 wt%).

The bulk stripping solution pH and the concentration of the ionic reactant solution added (C^{add}) are relatively easily adjustable parameters, which can be used to influence mass transfer enhancement. The feasible pH operating range (1–13) is a compromise between driving force maximization and membrane polymer stability under extreme pH conditions. Otherwise, maximum enhancement is simply achievable by a stripping solution pH higher than 14. The stripping solution pH is related to the stripping solution bulk concentration of the ionic reactant ($B_{s,b}$) via Eq. (25), for the extraction of organic acid or base, respectively:

$$B_{s,b} = \frac{10^{pH}}{K_w} = 10^{pH-14} \quad \text{and} \quad B_{s,b} = 10^{-pH}. \tag{25}$$

During the extraction an ionic reactant solution, sodium hydroxide or hydrochloric acid, is added to the stripping solution to neutralize the extracted organic acid or base, respectively, and maintain the pH at a constant value. The total molar organic concentration of the stripping solution at steady state, $C_{s,b}^T$ (i.e. $A_{s,b}$ plus $AB_{s,b}$), is entirely controlled by the concentration of this ionic reactant solution (C^{add}) and can be calculated from Eq. (26).

$$C_{s,b}^T = \frac{1000.\rho_s}{\left(\frac{Mw_{add}}{Mw_A}.\frac{100}{C^{add}\ (wt\%)} + 1\right) Mw_A}. \tag{26}$$

The concentration of the organic in each of the forms ($A_{s,b}$ and $AB_{s,b}$) is a function of the ionic reactant concentration ($B_{s,b}$) at the bulk stripping solution, and is therefore controlled by the stripping solution pH.

$$A_{s,b} = \frac{C_{s,b}^T}{1 + K.B_{s,b}}. \tag{27}$$

For phenol neutralization, typically 2.5 M caustic solution is added which results in a stripping solution total organic concentration of 2 M. This value is well above the phenol solubility in distilled water of 0.85 M, and in the MARS aqueous

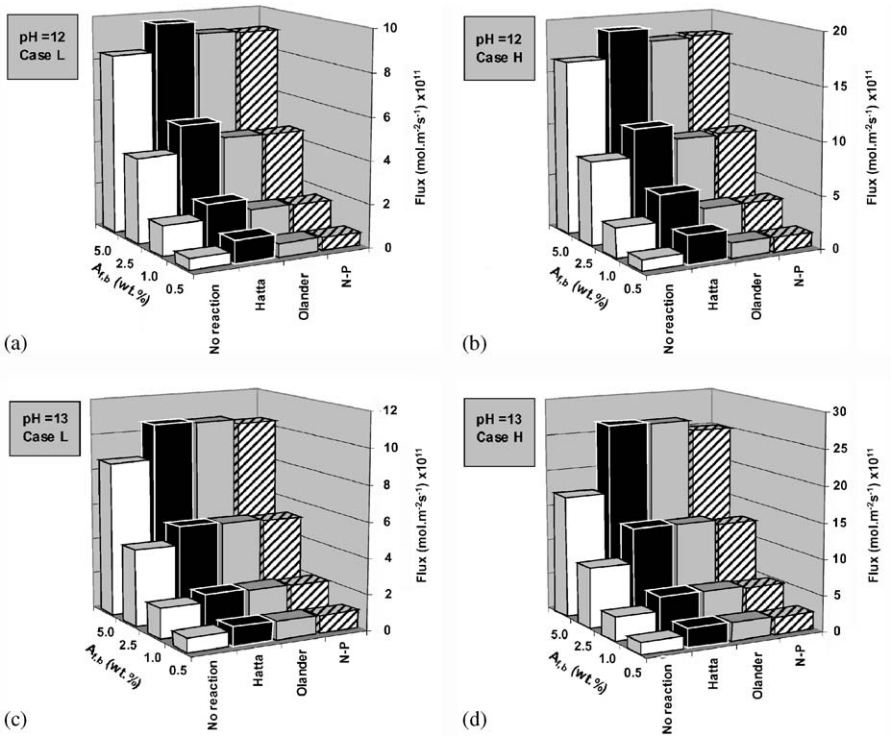

Fig. 3. (a)–(d) Comparison of fluxes calculated by different models for two different pH values and for two membrane permeabilities (H and L).

saline layer of about 0.35 M, respectively (Han et al., 2001), and allows the concentrated organic to be recovered.

5. Model simulations

5.1. Overview of model results: comparison of calculated fluxes

Figs. 3 (a)–(d) summarises the organic fluxes calculated from the three models for a wide range of operating conditions: the two membrane permeability case studies (*H* and *L*), and two stripping solution pH values (12 and 13),with a range of bulk feed concentrations from 0.5 to 5 wt%. A list of the input parameters values used is presented in Table 1. Flux values calculated from the N–P model were obtained by numerically solving the system of differential equations (Eqs. (7)–(10) plus boundary conditions) using the gPROMs dynamic simulator (Process System Enterprise Ltd., 1999). The Olander model fluxes were calculated from Eqs. (11) to (15). The Hatta model fluxes were calculated from Eqs. (19) to (21). Finally,the fluxes for mass transfer without chemical reaction were calculated from Eqs. (11) to(13), assuming an enhancement factor (E) equal to one.

All the simulations were run for phenol extraction in a caustic stripping solution, therefore the neutral organic (A) in these models simulations is phenol, the ionic reactant (B) is hydroxide, the ionic product is phenolate (AB) and the counter ion (C^*) is sodium.

Results in Fig. 3 show that each of the three models predicts higher mass transfer fluxes compared to the phenol fluxes calculated by neglecting chemical reaction enhancement. As is expected, the mass transfer enhancement is more pronounced for higher stripping solution pH. At pH 12, the Hatta model predicts a significantly higher mass transfer than Olander and N–P models. At pH 13 Hatta and Olander models predict similar fluxes for both membrane permeabilities, but the N–P model predicts slightly lower phenol fluxes, especially for the case study *H*.

For better quantification of these phenomena flux ratios were also considered. In order to quantify the effect of chemical reaction reversibility on mass transfer, the Hatta/Olander flux ratios for the same conditions were calculated. On the other hand the N–P/Olander fluxes ratio quantifies the electric potential contribution. Both flux ratios are presented in Table 2. For low feed bulk phenol concentrations ($A_{f,b}=0.5$ and 1.0 wt%) and stripping solution pH=11, the neutral phenol concentration in the stripping solution ($A_{s,b}=1.73$ wt%) becomes higher than $A_{f,b}$ and therefore the concentration driving force for mass transfer becomes negative, leading also to the negative organic fluxes reported in Tables 2 and 3, i.e. the organic flux changes its' direction from the stripping solution toward the feed solution.

5.2. Comparison between N–P and Olander models

The N–P model takes into account concentration and electric driving forces for the mass transfer of charged species

Table 2
Flux ratios calculated by different models for two different pH values and membrane permeabilities

$A_{f,b}$ (wt%)	pH		
	11	12	13
(a) Flux ratio N–P/Olander L = Low flux membrane ($k_g = 2 \times 10^{-7}$ m s^{-1})			
0.5	flux < 0	0.98	0.97
1	flux < 0	0.98	0.97
2.5	1.05	0.99	0.98
5	1.01	0.99	0.98
(b) Flux ratio N–P/Olander H = High flux membrane ($k_g = 5 \times 10^{-7}$ m s^{-1})			
0.5	flux < 0	0.96	0.94
1	flux < 0	0.98	0.94
2.5		1.01	0.95
5	1.01	1.01	0.95
(c) Flux ratio Hatta/Olander L = Low flux membrane ($k_g = 2 \times 10^{-7}$ m s^{-1})			
0.5	flux < 0	1.70	1.04
1	flux < 0	1.31	1.02
2.5	3.30	1.18	1.01
5	1.54	1.07	1.00
(d) Flux ratio Hatta/Olander H = High flux membrane ($k_g = 5 \times 10^{-7}$ m s^{-1})			
0.5	flux < 0	1.87	1.04
1	flux < 0	1.51	1.02
2.5	3.29	1.15	1.01
5	1.54	1.07	1.01

Table 3
Ratios of driving forces and overall mass transfer coefficients calculated and used to predict fluxes by Hatta and Olander models

$A_{f,b}$ (wt%)	pH		
	11	12	13
(a) Driving force ratio Hatta/Olander			
0.5	flux < 0	1.60	1.04
1	flux < 0	1.23	1.02
2.5	3.25	1.08	1.01
5	1.53	1.04	1.00
(b) K_{ov} ratio Hatta/Olander for L = Low flux membrane ($k_g = 2 \times 10^{-7}$ m s^{-1})			
0.5	flux < 0	1.06	1.00
1	flux < 0	1.07	1.00
2.5	1.02	1.09	1.00
5	1.01	1.03	1.00
(c) K_{ov} ratio Hatta/Olander for H = High flux membrane ($k_g = 5 \times 10^{-7}$ m s^{-1}			
0.5	flux < 0	1.16	1.00
1	flux < 0	1.22	1.00
2.5	1.01	1.06	1.00
5	1.01	1.03	1.00

(*B* and *AB*), whereas the Olander model considers only the concentration driving force.

Fig. 3 shows that for the simulation input range chosen, the incorporation of the Nernst–Planck effect does not have a major effect on the predicted phenol flux. From this result it is possible to advocate the hypothesis that the concentration driving force rules the mass transfer, and the electric field driving force contribution is not important in this system. In what follows we will try to explain this result.

The values of the electric field in the stripping solution liquid film, calculated from the N–P model, are shown in Fig. 4, and are of the same order of magnitude as those found in the literature for similar cases (Dammak et al., 1999). The flux equation (Eq. (1)) for each of the ionic species consists of two components, flux generated due to the concentration driving force, and flux generated due to the electric field driving force. The induced electric field is negative and according to Eq. (1) for the hydroxide ion it generates hydroxide flux in a direction opposing the concentration driving force. As a result, the total hydroxide flux from the bulk stripping solution toward the membrane surface decreases. Consequently, the chemical reaction enhancement

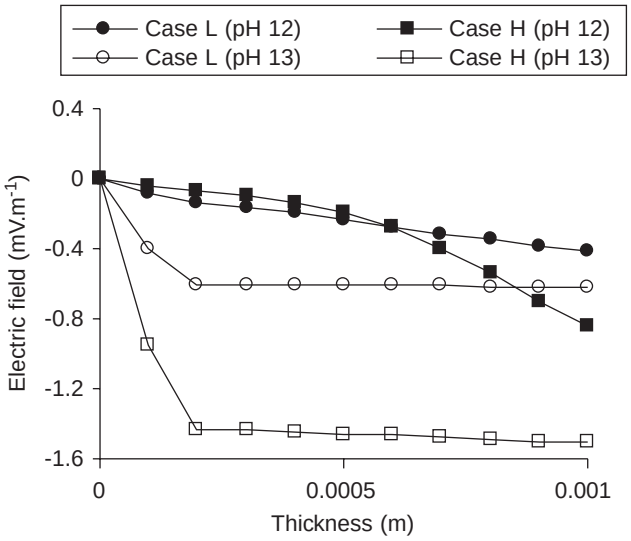

Fig. 4. Electric field within the stripping solution liquid film. (The symbols used are only for legend indication and are not related to any experimental data).

factor is smaller and the phenol flux lower. This effect is more evident at pH 13 (the electric field has higher values, Fig. 4) where the predicted by the N–P model flux is found to be lower than the one predicted by the Olander model (see Table 2). On the other hand for the phenolate ion the electric field and the concentration gradient fluxes have the same directions, and thus it follows that the total phenolate flux in this case should be accelerated. Thus the electric field serves to slow the diffusion of the more mobile hydroxide ion, while speeding up the transfer of the less mobile phenolate ion. However, the resulting overall flux is less than 5% different from to the flux calculated from the Olander expression (Table 2).

Concentration profiles for each of the species along the stripping liquid film were also calculated using the N–P and the Olander models for both membrane permeability case studies (L and H) at pH 12 and 13. The differences between these concentration profiles are negligible. Results for case study H, where the highest divergence between fluxes was observed, are presented in Fig. 5. Note that the phenolate (AB) concentration scale in Fig. 5 is amplified and the observed difference in the phenolate concentrations predictions is actually also within 5%. In general, the inclusion of the ionic interactions into the mass-transfer model for the system has less than 5% impact on the mass transfer fluxes. Therefore the Nernst–Planck effect, under these conditions is not really important for the MARS mass-transfer calculations. The Olander model is accurate enough for the MARS process operations predictions and design. Its mathematical simplicity, especially in light of the proposed analytical solution, makes it a preferable choice for MARS process description.

5.3. Comparison between Hatta and Olander models: driving force and mass transfer resistances

As illustrated in Fig. 3 and Tables 2c and 2d, the fluxes estimated from the Hatta model can be nearly 1.7 times higher than those obtained from the Olander model. The differences between the two model predictions are more pronounced for lower feed bulk concentrations ($A_{f,b}$) and at pH near the phenol pK_a (see results at pH 12). In both models the organic fluxes can be expressed by Eq. (11), but in the Olander model the chemical reaction reversibility effects both terms of the flux equation, the mass transfer coefficient through the enhancement factor (Eq. (13)), and the driving force through the concentration of the neutral organic in the bulk stripping solution ($A_{s,b}$). Each of these effects will be quantified separately.

For the same input parameters, Hatta and Olander models use different driving force values. For the Hatta model $A_{s,b}$ always equals to zero, while in the Olander model this concentration can be calculated from Eqs. (26) to (27) and is a function of the stripping solution pH and concentration (i.e. $B_{s,b}$). As the stripping solution pH approaches the pK_a value, the chemical equilibrium shifts towards the reagents, and therefore the concentration of the neutral organic in the bulk stripping solution increases, leading to lower driving forces.

A comparison between the driving forces used in the Hatta and Olander models at different pH is made in Fig. 6 and in Table 3a. Fig. 6 shows that for a stripping solution at pH 13, the driving forces differences are within 5%, and therefore applying Hatta model driving force is a fairly good assumption. However for a stripping solution at pH 12, depending on the concentration of the bulk feed solution ($A_{f,b}$), the ratio between these driving forces can be as high as 1.60 (Table 3a).

The same trend for discrepancy between Hatta and Olander model predictions as a function of pH was found for the organic fluxes (Tables 2c and 2d). This result suggests that the predicted fluxes differences are mainly due to the different driving forces used by each of the models. However, it is still important to verify the effect of the chemical reaction on the overall mass transfer coefficient in order to assess if the flux differences are entirely quantified by the driving force differences. The overall mass transfer coefficients were calculated according to Olander (Eqs. (13)–(15)) and Hatta (Eqs. (13), (16) and (17)) models for stripping solution pH of 12 and 13, and for both membrane permeability cases study. The results presented in Tables 3b and 3c show that, at pH 12, the chemical reaction reversibility also has an important effect on the stripping solution liquid film mass transfer coefficient. In this case the flux differences between Olander and Hatta models cannot be explained only on the basis of driving force, but also on the basis of the mass transfer coefficient enhancement effects. Further discussion on this issue will be presented in the next section.

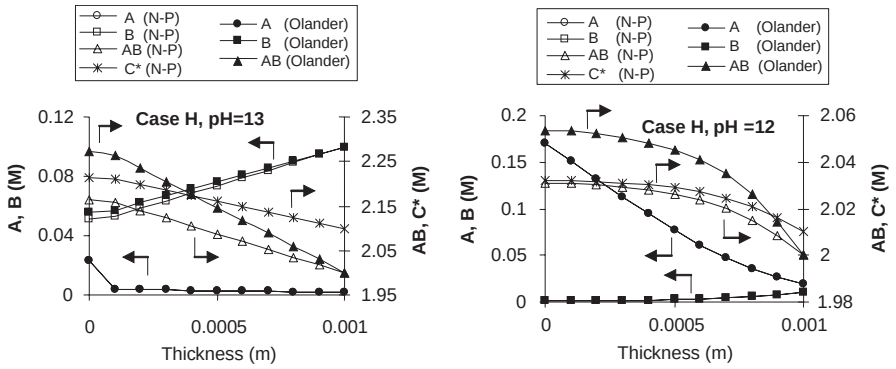

Fig. 5. Comparison of species concentration profiles in the stripping solution liquid film calculated by N–P and Olander models for a feed concentration of 5 wt% phenol. (The symbols used are only for legend indication, and are not related to any experimental data).

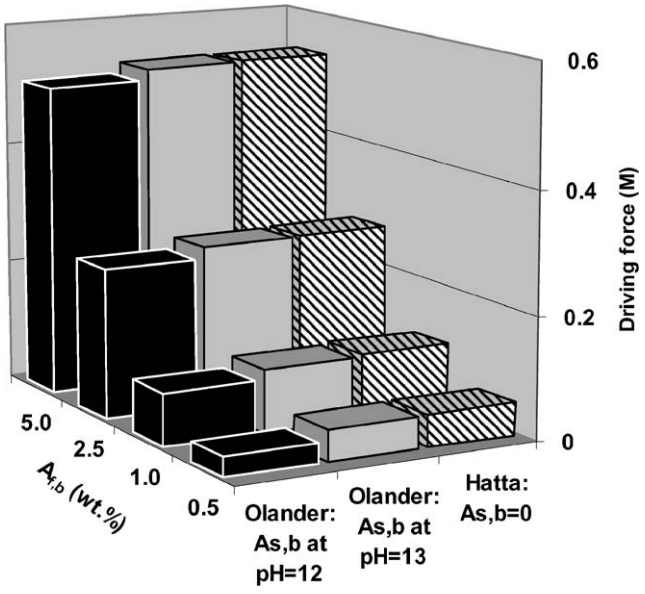

Fig. 6. Driving forces for different feed concentrations, following the Olander and Hatta models.

5.4. Comparison between Hatta and Olander models: concentration profiles

Fig. 7(a and b) shows concentration profiles calculated using Olander and Hatta models. As expected, the Hatta model generates rectilinear concentration profiles, as shown in Fig. 7a for pH 12. As phenol (A) diffuses towards the bulk stripping solution it reacts with the hydroxide (B) diffusing in the opposite direction, and is completely converted to phenolate (AB).

The hydroxide concentrations in the bulk stripping solution, and thus the hydroxide driving forces, are equal for both membrane case studies, shown in Fig. 7a. However the more permeable membrane (case study *H*), generates higher phenol fluxes toward the stripping solution (see Fig. 3). Consequently the hydroxide is consumed nearer to the stripping solution bulk and the reaction plane is shifted away from the membrane surface, from a liquid film thickness position

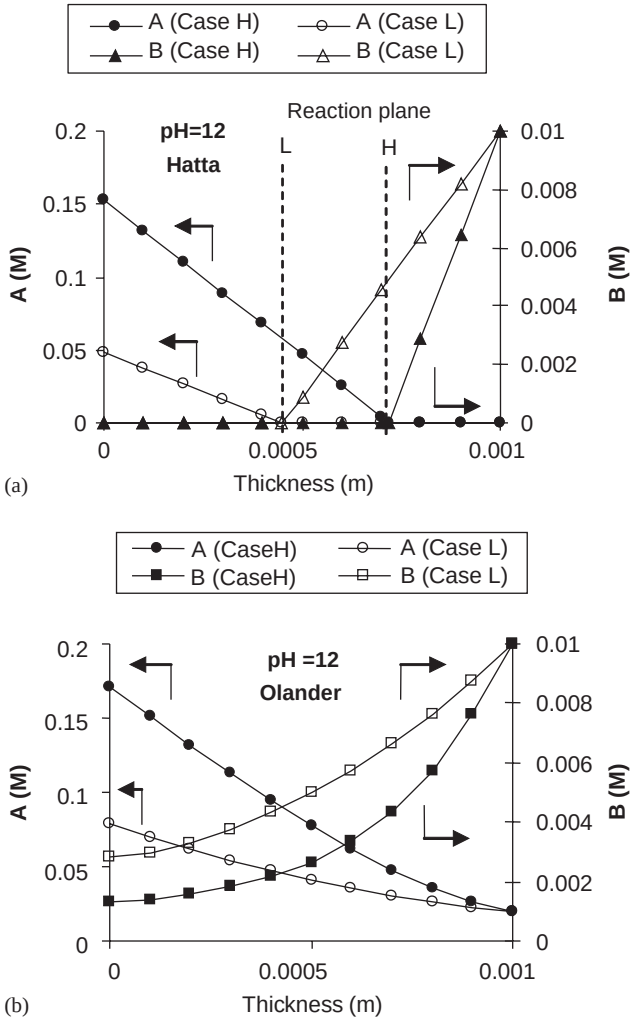

Fig. 7. (a and b) Comparison of species concentration profiles within the stripping solution liquid film for the two membrane permeability cases at pH 12 and $A_{f,b}$ of 5 wt%. Calculations by Hatta and Olander model in Figs. 7a and 7b, respectively. (The symbols used are only for legend indication and are not related to any experimental data).

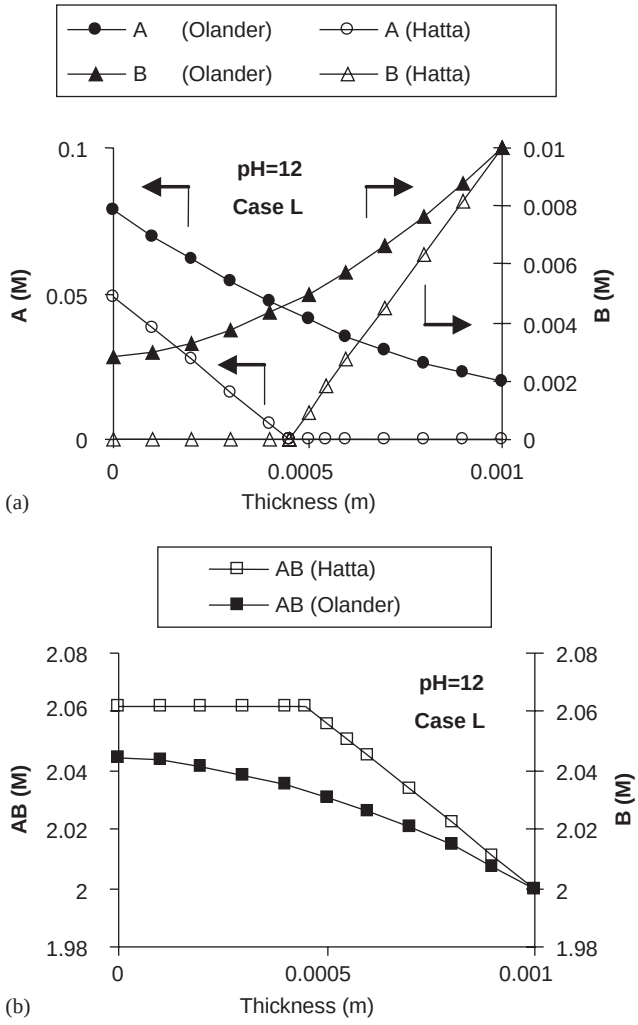

Fig. 8. (a and b) Comparison of reagents and product concentration profiles within the stripping solution liquid film, calculated by Hatta and Olander models for the low permeability membrane case (L), at pH 12 and 5 wt% phenol in feed. (The symbols used are only for legend indication and are not related to any experimental data).

of 0.45 mm to a position of 0.72 mm (Fig. 7a). As a result the chemical reaction enhancement factor is lower than in the case study *L*. The chemical reaction enhancement factor reduction is more pronounced in Eq. (16), containing the ratio $B_{s,b}/A_{s,i}$ which is dramatically reduced in case study *H*.

In contrast, the Olander model does not assume that the chemical reaction takes place at any specific point of the liquid film; instead it assumes an instantaneous chemical equilibrium alongside the whole stripping liquid film. Due to reaction reversibility, all the concentration profiles become curvilinear and none of the concentrations of the reacting species is zero at any point in the liquid film. Figs. 8a and b give a direct comparison between the calculated Hatta and Olander concentration profiles for the case study *L* at pH 12. The reverse chemical reaction step in the Olander model implies that the phenol concentration gradient is diminished (Fig. 8a) and so is the respective phenol flux. Thus the reverse step slows down phenol mass transfer.

Concentration profiles for both membrane cases study calculated using the Olander model are shown in Fig. 7b, and they exhibit similar trends to those calculated from the Hatta model. Higher phenol and lower hydroxide concentrations were obtained at the membrane/stripping solution interface and alongside the stripping liquid film for case study *H* as compared with case study *L*. Similarly to the Hatta model, the Olander model predicts lower chemical reaction enhancement for case study *H* due to the lower $B_{s,b}/A_{s,i}$ (hydroxide/phenol) ratio (Eq. (14)). The concentration profiles generated by the Olander model, assuming they are similar to the actual concentrations in the MARS process, provide us with important additional information. Since hydroxide is consumed by the chemical reaction, its concentration at the membrane/stripping interface is actually lower than in the bulk stripping solution, thereby reducing the pH at the interface. This should result in a lower rate of membrane degradation than would occur at bulk solution conditions. A longer operating membrane lifetime could result in an important savings for the industrial process.

5.5. The Hatta model as a particular case of the Olander model

Since the Hatta model requires a lower number of parameters and is mathematically simpler than the Olander one, it is interesting to assess when this model can be used accurately for the MARS process mass transfer predictions. As we already mentioned the reversible chemical reaction affects both elements contributing to the phenol flux (Eq. (11)), the overall mass-transfer coefficient, and the driving force. Hence the two important equations to be analysed are:

$$A_{s,b} = \frac{AB_{s,b}}{K.B_{s,b}} \to 0 \tag{28}$$

$$E = 1 + \frac{D_{AB}}{D_A}.\frac{K.B_{s,b}}{1 + \frac{D_{AB}}{D_B}K.A_{s,i}} \overset{\frac{D_{AB}}{D_B}.A_{s,i}.K \gg 1}{\to} 1 + \frac{D_B}{D_A}.\frac{B_{s,b}}{A_{s,i}}. \tag{29}$$

As can be seen from the above equations, the first case when the Hatta model can be applied accurately corresponds to equilibrium constants (K) high enough to ensure that at operating stripping pH the neutral organic in the bulk stripping solution is negligible and the Olander enhancement factor tends asymptotically to the Hatta value. To illustrate this we have calculated the Hatta model concentration profiles shown in Figs. 8a and b, using the numerical solution for the Olander model, but assuming an equilibrium constant of 10^{10} instead of $10^4\ M^{-1}$. Indeed for compounds with high equilibrium constants the chemical reaction reverse step becomes negligible, which results in a well-defined reaction front and rectilinear concentration profiles.

There is a second case where Hatta analysis can be useful. When the equilibrium constant has an intermediate value ($10^4\,M^{-1}$) (for example phenol extraction at pH 13), but the ionic reactant concentration (e.g. hydroxide) in the bulk stripping solution is high enough to shift the chemical reaction equilibrium towards the product (see Eq. (28)), the neutral organic concentration in the bulk stripping solution is negligible compared to the driving force (Table 3a). For the particular set of parameters and concentrations used in this study, for phenol at pH 13, the reaction reversibility has a negligible effect on the overall mass-transfer coefficient (Tables 3b and 3c), however this may not be true for other combinations of input parameters and Hatta and Olander enhancement factors still may be different.

In some cases a hybrid model could be used, when the reverse step of the chemical reaction has negligible effect on the overall mass transfer coefficient, but the neutral organic in the bulk stripping solution is still significant for the bulk driving force ($A_{f,b} \sim A_{s,b}$). In spite of the mathematical contradiction, such a hybrid model could use a driving force from the Olander model, and an overall mass transfer coefficient calculated from the Hatta model enhancement factor. This model has the advantage of using an accurate driving force, and retaining the mathematical simplicity of the Hatta model.

The last limiting case when both models predict an equal mass transfer coefficient enhancement, takes place when the stripping liquid film resistance is completely eliminated and the mass transfer enhancement is maximum. In such a scenario the membrane and the feed liquid film resistances are only important for mass transfer and the organic flux can easily be calculated from Eq. (11), replacing K_{ov} with k_g. However the reaction reversibility still has to be considered in the driving force term.

The systematisation of the above scenarios gives a better understanding of when and why the chemical reaction reversibility is important, however its practical application is rather limited. It is difficult to assess exactly at which conditions (e.g. concentrations and stripping solution pH values) the reaction can be assumed irreversible, and so when the Hatta model or hybrid model can be accurately applied. Therefore, we recommend that the Olander model is used for analysis of the MARS process.

6. Conclusions and generalizations

Mass transfer rate in the MARS process was mathematically described in this study using three different mathematical models: the N–P model which takes into account the chemical reaction reversibility and Nernst–Planck effects on the mass transfer enhancement by a second-order instantaneous chemical reaction; the Olander model which takes into account only the chemical reaction reversibility, and the Hatta model which considers the chemical reaction to be irreversible. Comparison of the fluxes calculated by the three models suggests that the Nernst–Planck effect has negligible influence on mass transfer under the MARS process operating conditions. In some particular cases it could be responsible for minor organic flux reduction, but the complexity of the model makes it less useful for engineering calculations.

Different cases when Olander and Hatta models predict similar organic fluxes, and so for which the chemical reaction can be assumed irreversible were identified. However chemical reaction reversibility is often important for mass transfer enhancement predictions, especially for the cases where the stripping solution pH is not very far from the pK_a value of the organic acid. For example, calculations presented in this paper show that the extraction of phenol ($pK_a = 10$) to a typical MARS stripping solution at pH 13 could be accurately predicted by the Hatta model. However, at pH 12 the chemical reaction reversibility has to be taken into account and application to the Olander model is required.

The Hatta model is quite attractive due to the lower number of parameters and its mathematical simplicity. Generally it can be used for predictions of mass transfer of organic acids or bases with high equilibrium constants, and for high concentration driving forces at extreme pHs. However it is difficult to assess exactly at which operating conditions the chemical reaction reversibility becomes important. Therefore the authors recommend the use of the Olander model for the MARS, and similar processes design calculations. Moreover, an analytical solution for the Olander model was developed in this paper to assist in such calculations.

Notation

A	transported solute, neutral, e.g. phenol, $mol\,m^{-3}$
AB	reaction product, monovalent, e.g. phenolate, $mol\,m^{-3}$
B	ionic reactant, monovalent, e.g. hydroxide, $mol\,m^{-3}$
C	concentration, $mol\,m^{-3}$
C^*	counter ion, monovalent, e.g. sodium, $mol\,m^{-3}$
D	diffusion coefficient, $m^2\,s^{-1}$
D_m	diffusion coefficient of neutral organic in membrane material, $m^2\,s^{-1}$
E	enhancement factor of mass transfer in stripping liquid film
F	Faraday constant $= 9.65.10^4\,C\,mol^{-1}$
I_m	membrane area, m^2
J	flux, $mol\,s^{-1}$
k_f	feed liquid film mass transfer coefficient, $m\,s^{-1}$
k_g	grouped mass transfer coefficient, $m\,s^{-1}$
k_m	membrane mass transfer coefficient, $m\,s^{-1}$
k_s	stripping liquid film mass transfer coefficient, $m\,s^{-1}$
K	Equilibrium constant, M^{-1}
K_a	organic acid dissociation constant, M^{-1}

K_b	organic base dissociation constant, M^{-1}
K_{ov}	overall mass transfer coefficient, $m\,s^{-1}$
K_p	partition coefficient of neutral organic between membrane and aqueous phase
K_w	water auto-ionisation constant, M^2
M_w	molecular weight, $g\,mol^{-1}$
R	gas constant $= 8.314\,J\,mol^{-1}\,K^{-1}$
RT/F	25.693 mV at 298.15 K
T	temperature, K
V	electric field, $V\,m^{-1}$
x	space dimension in stripping liquid film thickness, m
z	specie charge, dimensionless

Greek letters

Ψ	electrical field term $= V.F/R.T$, m^{-1}
δ_m	membrane thickness, m
ϕ	molar flux per membrane area, $mol\,m^{-2}\,s^{-1}$
ρ_s	stripping solution density, $kg\,m^{-3}$

Subscripts and superscripts

add	added ionic reactant, sodium hydroxide for organic acid extraction or hydrochloric acid for organic base extraction
b	in the bulk of the solution
f	feed solution
i	at membrane/stripping solution interface
j	specie index
0	in the absence of chemical reaction
ov	overall
s	stripping solution, reactant phase
T	total organic, neutral (A) plus ionic (AB) forms

Acknowledgements

This work was funded by the UK Engineering and Physical Sciences Research council (EPSRC) Grant GR/R57188/01. F.C. Ferreira acknowledges financial support from Fundação para a Ciência e Tecnologia, Grant PRAXIS XXI/BD/21448/99.

Appendix A

A.1. Derivation of the N–P Model: reversible second order reaction with ionic mobility (Nernst–Planck effect)

This model uses flux Eq. (1), which takes into account both concentration and electric driving forces. A mass balance is made on each of three species (A, B, AB) within the stripping solution liquid film, from the membrane/stripping solution interface ($x = 0$) to the stripping liquid film/bulk interface ($x = \delta$) (note that all the equations are derived for planar coordinates). These mass balances equations assume steady state fluxes and take into account species consumption or production by the chemical reaction ($\Gamma = k.A.B - k^{-1}.AB$):

$$0 = -\frac{dJ_A}{dx} - \Gamma, \tag{A.1}$$

$$0 = -\frac{dJ_B}{dx} - \Gamma, \tag{A.2}$$

$$0 = -\frac{dJ_{AB}}{dx} + \Gamma. \tag{A.3}$$

The chemical reaction considered in this work is an equimolar reaction. Γ can be eliminated from the above equations, thus:

$$-\frac{dJ_A}{dx} - \frac{dJ_{AB}}{dx} = 0 \Rightarrow D_A.\frac{d^2A}{dx^2} + D_{AB}.\frac{d^2AB}{dx^2} - z_{AB}.D_{AB}.\frac{d(\Psi.AB)}{dx} = 0, \tag{A.4}$$

$$-\frac{dJ_B}{dx} - \frac{dJ_{AB}}{dx} = 0 \Rightarrow D_B.\frac{d^2B}{dx^2} - z_B.D_B.\frac{d(\Psi.B)}{dx} + D_{AB}.\frac{d^2AB}{dx^2} - z_{AB}.D_{AB}.\frac{d(\Psi.AB)}{dx} = 0. \tag{A.5}$$

Note that the specie A is neutral, hence is not affected by the electric field ($z_A = 0$). The counter ion is not consumed or produced during the reaction and its concentration is eliminated from the final model equations using electroneutrality Eq. (3). By substituting Eq. (3) into Eq. (5) one can obtain the following equation for the electric field:

$$\Psi = z_{C^*}.\frac{\frac{dB}{dx}(D_{C^*} - D_B) + \frac{dAB}{dx}(D_{C^*} - D_{AB})}{B.(D_{C^*} + D_B) + AB.(D_{C^*} + D_{AB})}. \tag{A.6}$$

In order to acknowledge chemical reaction reversibility, the chemical equilibrium relation is imposed along the stripping liquid film:

$$AB = K.B.A. \tag{A.7}$$

The boundary conditions for the above system are as following:

$$A(\delta) = A_{s,b}, \tag{A.8}$$

$$B(\delta) = B_{s,b}, \tag{A.9}$$

$$A(0) = A_{s,i}, \tag{A.10}$$

$$AB(\delta) = K.A_{s,b}.B_{s,b}, \tag{A.11}$$

$$-D_B.\frac{dB(0)}{dx} + z_B.D_B.B(0).\Psi(0) - D_{AB}.\frac{dAB(0)}{dx} + z_{AB}.D_{AB}.AB(0).\Psi(0) = 0, \tag{A.12}$$

$$J_A(0) = J_A(\delta) + J_{AB}(\delta) \Rightarrow -D_A.\frac{dA(0)}{dx} = -D_A.\frac{dA(\delta)}{dx} - D_{AB}.\frac{dAB(\delta)}{dx} + z_{AB}.D_{AB}.AB(\delta).\Psi(\delta), \tag{A.13}$$

$$J_g = J_A(0) \Rightarrow k_g.(A_{f,b} - A_{s,i}) = -D_A.\frac{\mathrm{d}A(0)}{\mathrm{d}x}, \qquad (A.14)$$

where

$$\Psi(z) = z_{C^*}.\frac{\frac{\mathrm{d}B(x)}{\mathrm{d}x}(D_{C^*} - D_B) + \frac{\mathrm{d}AB(x)}{\mathrm{d}x}(D_{C^*} - D_{AB})}{B(x).(D_{C^*} + D_B) + AB(x).(D_{C^*} + D_{AB})}$$

and $x = 0$ at the membrane/stripping solution interface; $x = \delta$ at the stripping liquid film/bulk solution interface. Eq. (A.11) reflects the chemical reaction equilibrium. Eq. (A.12) reflects the membrane impermeability to ionic species. Eqs. (A.13) and (A.14) are steady state fluxes mass balances at each of the stripping liquid film interfaces.

A.2. Derivation of the Olander model: reversible second-order reaction for neutral species

The Olander model is a simplification of the N–P model, in which it is assumed that all species are neutral ($z = 0$) and the electrical potential is also zero. Therefore Olander model equations can be obtained from Eqs. (A.4), (A.5) and (A.7), assuming $z_{AB} = 0$ in Eq. (A.4) and $z_B = 0$ and $z_{AB} = 0$ in Eq. (A.5). Eqs. (A.8)–(A.14) are also used in Olander model as boundary conditions. However in Olander model, z_{AB} is assumed to be zero in Eq. (A.13) and z_B and z_{AB} are assumed to be zero in Eq. (12). The numerical solution of the obtained system of equations allows the calculation of organic fluxes and species concentrations profiles along the stripping liquid film.

Olander had solved this system of differential equations and expressed the organic flux (Eq. (11)) as a function of the overall mass transfer coefficient (Eq. (13)) and the bulk concentration driving force. This solution contains the chemical reaction enhancement factor (Eq. (14)), which is a function of the organic concentration at the interface between the inert and the reactant phases. However, for several systems this concentration is not expressed explicitly in terms of measurable variables.

In what follows we will present an analytical solution of the Olander model applied to the MARS process. The two organic fluxes are re-defined; a flux from the bulk/liquid film wastewater interface to the membrane/stripping solution interface (ϕ_g) and an organic flux from the membrane/stripping solution interface to the liquid film/bulk stripping solution interface (ϕ_s). At steady state this two organic fluxes (ϕ_g, ϕ_s) should be equal.

$$\begin{aligned}\phi_{\mathrm{ov}} = \phi_s = \phi_g &\Leftrightarrow k_g(A_{f,b} - A_{s,i}) \\ &= E.k_s^0(A_{s,i} - A_{s,b}).\end{aligned} \qquad (A.15)$$

Hence, one can obtain the expression for the interfacial concentration:

$$A_{s,i} = \frac{k_g.A_{f,b} + E.k_s^0 A_{s,b}}{E.k_s^0 + k_g}. \qquad (A.16)$$

Substituting Eq. (13) in the above equation, the enhancement factor can be eliminated and a quadratic equation with $A_{s,i}$ as unknown is obtained. This quadratic equation has two mathematical solutions but one of them always generates a negative value and therefore only one of the solutions for $A_{s,i}$ (shown in Eq. (15)) has a physical meaning.

A.3. Derivation of the Hatta model: irreversible second-order reaction

Hatta had defined an enhancement factor (E) for the reactant solution liquid film based on the following assumptions: (i) second order instantaneous irreversible reaction; (ii) the two reagents never coexist in the liquid stripping film; (iii) the two reagents are instantaneously and completely consumed at the reaction front. Hence, the bulk stripping solution organic neutral concentration ($A_{s,b}$) is assumed to be zero and the enhancement factor defined in Eq. (16) for this case is substituted in the equations for ϕ_s.

$$\phi_s = E.k_s^0 A_{s,i} = \left(1 + \frac{D_B}{D_A}.\frac{B_{s,b}}{A_{s,i}}\right).k_s^0 A_{s,i}. \qquad (A.17)$$

At steady state ϕ_g and ϕ_s should be equal (see Eq. (A.15) for ϕ_g definition) and Eq. (A.18) can be obtained to calculate ($A_{s,i}$):

$$A_{s,i} = \frac{\frac{k_g}{k_s^0}.A_{f,b} - \frac{D_B}{D_A}.B_{s,b}}{\left(1 + \frac{k_g}{k_s^0}\right)}. \qquad (A.18)$$

Replacing Eq. (A.18) back in Eq. (A.17), the enhanced flux can be calculated by the expression:

$$\begin{aligned}\phi_{\mathrm{ov}} &= \frac{1}{\left(\frac{1}{k_g} + \frac{1}{k_s^0}\right)}.\left[A_{f,b} + \frac{D_B}{D_A}.B_{s,b}\right] \\ &= K_{\mathrm{ov}}^0.\left[A_{f,b} + \frac{D_B}{D_A}.B_{s,b}\right] = K_{\mathrm{ov}}.A_{f,b}.\end{aligned} \qquad (A.19)$$

Rearranging Eq. (A.19), Eq. (18) is obtained.

References

Al-Marzouqi, M.H., Hogendoorn, K.J.A., Versteeg, G.F., 2002. Analytical solution for facilitated transport across a membrane. Chemical Engineering Science 57, 4817–4829.

Astarita, G., Savage, D.W., 1982. Simultaneous absorption with reversible instantaneous chemical reaction. Chemical Engineering Science 37 (5), 677–686.

Brian, P.L.T., Baddour, R.F., Matiatos, D.C., 1964. An ionic penetration theory for mass transfer with chemical reaction. A.I.Ch.E. Journal 10 (5), 727–733.

Chin, K., 2003. MARS technology debuts in the UK. Chemical Engineering Progress 99 (4), 13.

Cussler, E.L., 1997. Diffusion-mass transfer in fluid systems, Cambridge University Press, Cambridge.

Dammak, L., Larchet, C., Auclair, B., 1999. Theoretical study of the bi-ionic potential and confrontation with experimental results. Journal of Membrance Science 155, 193–207.

Ferreira, F.C., 2004. Membrane aromatic recovery system (MARS): theoretical analysis and industrial applications. Ph.D. Thesis, Imperial College, London.

Ferreira, F.C., Han, S., Livingston, A.G., 2002a. Recovery of Aniline from Aqueous Solution using the Membrane aromatic recovery system (MARS). Industrial and Engineering Chemistry, Research 41, 2766–2774.

Ferreira, F.C., Han, S., Boam, A.T., Zhang, S., Livingston, A.G., 2002b. Membrane aromatic recovery system (MARS): lab bench to industrial pilot scale. Desalination 148, 267–273.

Grosjean, P.R.L., Sawistowski, H., 1980. Liquid/liquid mass transfer accompanied by instantaneous chemical reaction. Transactions of Industrial and Engineering Chemistry, Research 58, 59–65.

Han, S., Ferreira, F.C., Livingston, A.G., 2001. Membrane aromatic recovery system (MARS): a new membrane process for the recovery of phenols from wastewaters. Journal of Membrane Science 188 (2), 219–233.

Hatta, S., 1928. Tohoku Imperial University Technical Reports, 8, 1.

Hatta, S., 1932. Tohoku Imperial University Technical Reports, 10, 119.

Noble, R.D., 1991. Analysis of ion transport with fixed site carrier membranes. Journal of Membrane Science 56, 229–234.

Olander, D.R., 1960. Simultaneous mass transfer and equilibrium chemical reaction. A.I.Ch.E. Journal 6 (2), 233–239.

Process System Enterprise Ltd. 1999. gProms Training Course.

Sherwood, T.K., Wei, J.C., 1955. Ion diffusion in mass transfer between phases. A.I.Ch.E. Journal 1 (4), 522–527.

Van Swaaij, W.P.M., Versteeg, G.F., 1992. Mass transfer accompanied with complex reversible chemical reactions in gas–liquid systems: an overview. Chemical Engineering Science 47 (13/14), 3181–3195.